

Photo-Degradation of Methylene Blue over V_2O_5 - TiO_2 Nano-Porous Layers Synthesized by Micro Arc Oxidation

M. R. Bayati · F. Golestani-Fard · A. Z. Moshfegh

Received: 15 October 2009 / Accepted: 16 November 2009 / Published online: 1 December 2009
© Springer Science+Business Media, LLC 2009

Abstract V_2O_5 - TiO_2 porous layers were synthesized via micro-arc oxidation for the first time. The effect of the applied voltage on morphology, composition, and photo-activity of the layers was investigated. The layers, which consisted of anatase, rutile, and vanadium pentoxide phases, revealed an enhanced photo-activity. About 93% of methylene blue solution was degraded on the synthesized layers after 120 min UV-irradiation with a reaction rate constant of $k = 0.0228 \text{ min}^{-1}$. The band gap energies of the vanadia-titania and pure titania layers were calculated as 2.56 and 3.39 eV, respectively.

Keywords Micro arc oxidation · Titanium oxide · Vanadium oxide · Catalysis

1 Introduction

Dyes are an important group of chemicals among different pollutants of ecosystem. They are utilized in various industries such as textile, paper, rubber, plastic, and cosmetic to color the products. These dyes are usually released in the industrial wastes, and, consequently discharged to the

surface waters. Dyes even in low concentration are visually detected and affect the aquatic life and food web; in addition, they are aesthetically displeasing. They can also inhibit sunlight into streams and affect the photosynthetic reactions [1]. Among the various types of dyes, methylene blue (MB) is one of the most commonly used substances for coloring cotton, wood, paper stocks, and silk. It is utilized in medicine as well. Severe exposure to MB will cause increased heart rate, vomiting, shock, Heinz body formation, cyanosis, jaundice and quadriplegia, and tissue necrosis in humans [2–4]. Due to these critical negative effects, MB should be eliminated from the human environment. The ways of treating the industrial wastes to eliminate hazardous pollutants have been reported by many scientists [5, 6]. Nowadays, heterogeneous photo-catalysis is the most efficient method for destroying organic pollutants in especially aqueous media [7–9]. This process is based on the use of ultraviolet or visible radiations to excite a semiconductor which on its surface the oxidation of the pollutants is performed.

Titanium dioxide is one of the important semiconductors which is widely used as an efficient photo-catalyst, because it is chemically and biologically inert, photo-catalytically stable, commercially available and inexpensive, and environmentally friendly. Although it has a lot of advantages including biological and chemical inertness, strong oxidizing power, cost-effectiveness, and long-term stability against photo-corrosion and chemical corrosion [10–17], its wide band gap ($\sim 3.2 \text{ eV}$) and electron-hole recombination limit its applications. Because of its wide band gap energy, it only absorbs the UV region of the solar spectrum which is about only 4% of the incoming solar energy. Therefore, numerous attempts have been directed to extend the absorption of TiO_2 towards the visible part of the spectrum by many researchers in the last three decades

M. R. Bayati · F. Golestani-Fard
Department of Metallurgical and Materials Engineering,
Iran University of Science and Technology,
P.O. Box 16845-161, Tehran, Iran

A. Z. Moshfegh (✉)
Department of Physics, Sharif University of Technology,
P.O. Box 11155-9161, Tehran, Iran
e-mail: moshfegh@sharif.ir

A. Z. Moshfegh
Institute for Nanoscience and Nanotechnology, Sharif University
of Technology, P.O. Box 14588-89694, Tehran, Iran

[18–20]. To decrease the charge recombination rate and increase the TiO₂ photo-catalytic efficiency, several methods have been put forward such as loading of metallic and non-metallic species [21, 22] inorganic ions [23, 24], noble and rare metals [25, 26] into the crystalline lattice of titania, or mixing titania with other semiconductor metal oxides [17, 27–30]. Such modifications can change TiO₂ surface properties by altering interfacial electron transfer process and, consequently, improve the photo-catalytic efficiency of the surface as compared with pure TiO₂.

While there are a variety of processes by which a TiO₂ layer can be produced, micro-arc oxidation (MAO) is considered to be appropriate for synthesizing such oxide layers. MAO is an electrochemical technique for formation of anodic films by spark/arc micro-discharges which move rapidly on the vicinity of the anode. This process is carried out at voltages higher than the breakdown voltage of the gas layer enshrouding the anode. Since the substrate is connected to positive pole of the rectifier as anode, the gas layer consists of oxygen. When the dielectric gas layer completely covers the anode surface, electrical resistance of the electrochemical circuit surges and the process continues providing that the applied voltage defeats the breakdown voltage of the gas layer. Applying such voltages leads to formation of electrical discharges via which electrical current could pass the gas layer. Due to strong electrical field (10^6 – 10^8 V m⁻¹) between anode and cathode, electrolyte anions are drawn into the structural pores where they can attend electrochemical reactions. Structural pores are formed by electron avalanches taking

places on the vicinity of the anode [31–38]. Characteristics of electrolyte have a great influence on the film formation kinetics. Phosphates, sulfates, silicates and borates are four conventional kinds of electrolytes employed in previous researches, and the formed TiO₂ films usually contain the element of the electrolytes (P, S, Si, B, etc.) [37].

There are only few reported researches on growing composite layers by MAO method, as listed in Table 1. Yerokhin and his group were the first group who synthesized Al₂O₃-TiO₂ composite layers [31]. Afterward, Wang et al. [39] produced a composite layer consisting of TiO₂ and SiO₂. Yan et al. [40] synthesized nano-structured Al₂O₃-ZrO₂ composite layers by MAO process. Finally, composite layers consisting of Al₂O₃, ZrO₂, and Y₂O₃ were made by Lou et al. [41]. All of these layers were produced for anti friction and wear applications. Very recently, He et al. prepared WO₃-TiO₂ composite photo-catalysts layers. They reported that about 85% of the methyl orange solution was decomposed on the composite layers after 10 h UV-irradiation [42].

V₂O₅ is one of the most important metal oxides catalysts with a narrow band gap and its mixture with TiO₂ can be useful for photo-catalytic reactions. To best of our knowledge, this is the first study on growth of V₂O₅-TiO₂ layers via MAO. Furthermore, sodium vanadate was utilized as MAO-electrolyte for the first time. In this research, we present results of growth, characterization, and photo-catalytic performance of V₂O₅-TiO₂ layers synthesized via MAO method under different applied voltages.

Table 1 Researches carried out on synthesizing composite layers via MAO method

System	Synthesis parameters					Application	Reference
	Substrate	Current type	Electrical parameters	Electrolyte	Temperature (°C)		
Al ₂ O ₃ -TiO ₂	Ti6Al4V	AC	–	NaAlO ₂ (0.05–0.2 M)	–	Tribology	[31]
SiO ₂ -TiO ₂	Ti6Al4V	Pulse DC	Voltage: 500 V	Na ₂ SiO ₃ (20.0 g/L), NaPO ₃ (6.0 g/L), NaAlO ₂ (4.0 g/L)	50	Tribology	[39]
Al ₂ O ₃ -ZrO ₂	Zr	Pulse DC	Voltage: 400 V Frequency: 100 Hz	NaAlO ₂ (0.3 M)	30	Tribology	[40]
Al ₂ O ₃ -ZrO ₂ -Y ₂ O ₃	Mg	AC	Anodic: 300 V, Cathodic: –60 V, Frequency: 700 Hz	NaAlO ₂ (0.12 M), K ₂ ZrF ₆ (0.035 M), Y(NO ₃) ₃ (0.002 M), KOH (0.089 M)	30	Corrosion	[41]
WO ₃ -TiO ₂	Ti	Pulse DC	Anodic voltage: 460 V, Cathodic voltage: 50 V, Frequency: 600 Hz	Na ₂ WO ₄ (10.0 g/L) NaOH (4.0 g/L) NaF (0.0–4.0 g/L)	24–40	Photocatalysis	[42]
V ₂ O ₅ -TiO ₂	Ti	DC	Voltage: 250–550 V	Na ₃ PO ₄ (10.0 g/L) NaVO ₃ (4.0 g/L)	70	Photocatalysis	This work

2 Experimental

A home-made rectifier with a maximum output of 600 V/30 A was used as the power supply for the growth process. 3 cm × 3 cm × 0.5 mm commercially pure titanium pieces, connected to the positive pole of the power supply as anode, were used as substrate. An ASTM 316 stainless steel cylindrical container, surrounding the substrates, was also used as cathode. Aqueous solutions containing Na₃PO₄·12H₂O (10 g L⁻¹, Merck) and NaVO₃ (4 g L⁻¹, Merck) were used as electrolyte. The electrolyte temperature was maintained at 70 ± 3 °C employing a water circulating system.

Prior to MAO treatment, substrates were cleaned in several steps including mechanical polishing followed by washing in distilled water. Afterward, the titanium plates were chemically etched in diluted HF solution (HF:H₂O = 1:20 Vol%) at room temperature for 30 s, and then washed in distilled water again. In the last stage of cleaning procedure, the substrates were ultrasonically cleaned in acetone for 15 min and finally washed by distilled water.

MAO treatment was carried out with applying DC voltages from 250 to 550 V in intervals of +50 V. The deposition time for each run was considered as 3 min.

Surface morphology of the layers was studied by scanning electron microscope (TESCAN, Vega II). Furthermore, X-ray diffraction (Philips, PW3710) and X-ray photoelectron spectroscopy (VG Microtech, Twin anode, XR3E2 X-ray source) techniques were employed to study phase structure and surface chemical composition of the synthesized layers.

In order to calculate the band gap energies (E_g) of the layers, a UV–Vis spectrophotometer (Carry 500) was used to measure the diffuse reflectance of the layers in a wavelength range of 200 to 500 nm. Afterward, the absorption was calculated according to the Kirchoff's law stating $\alpha + \rho + \tau = 1$, where α , ρ , and τ are absorptance, reflectance, and transmittance, respectively. It should be noted that the substrates were completely opaque. Hence, their transmittance was assumed to be zero, so $\alpha = 1 - \rho$. Then, the $d\alpha/d\lambda$ was calculated and plotted as a function of wavelength to find the wavelength at which the maximum

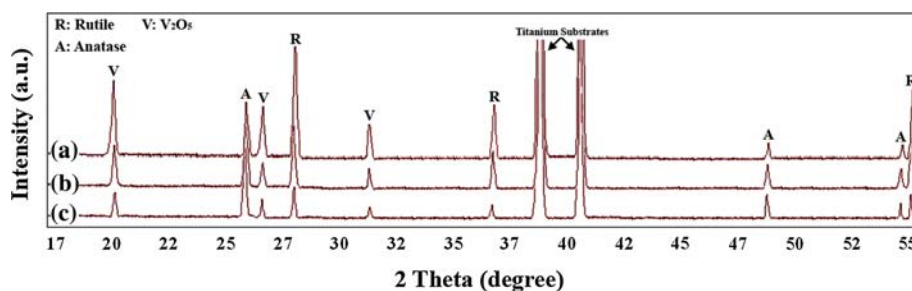
absorption occurs (λ_m). E_g can be calculated via the formula $E_g = hc/\lambda_m$ where C is the light speed in vacuum (2.99×10^8 m s⁻¹) and h is the Planck's constant (6.626×10^{-34} J s). Consequently, E_g (eV) = 1,236.56/ λ (nm).

The photo-catalytic activity of the layers was evaluated by measuring the degradation rate of aqueous methylene blue (MB) solution at room temperature. A UV–Vis spectrophotometer (Jascow Y-530) was used to measure the change in concentration, based on the Beer-Lambert equation stating $A = \varepsilon \times b \times C$ where A , ε , b , and C are absorption of the solution, molar absorptivity, path length, and solution concentration, respectively. Since b and ε are constant, the parameter C is linearly proportioned to the absorption; thus, it can be found by measuring the parameter A . To do that, 50 mL of the MB solution (50 ppm) and a 1 cm × 1 cm sample were placed in a quartz cell. A UV lamp (Philips, 25 W) was used as an irradiation source during photo-catalytic experiments. In each experiment, prior to UV irradiation, the solution and the catalyst were left in the dark for 60 min (as a reference point) until adsorption/desorption equilibrium was reached. The solution was then irradiated under UV light. A fixed quantity of the solution was removed every 20 min to measure the absorption and then the concentration. The absorptivity measurements were carried out at a fixed wavelength of 664 nm, because the maximum light absorption by the MB solutions occurs at this wavelength [43]. To make a comparison between the photo-catalytic activity of the synthesized composite layers and that of pure TiO₂ layers, three TiO₂ samples were grown utilizing sodium three-phosphate (10.0 g L⁻¹) as electrolyte under different applied voltages. A completely similar set of photo-catalytic experiments were carried out on these pure TiO₂ layers.

3 Results and Discussion

XRD patterns indicating formation of both the titanium and the vanadium oxides in the synthesized layers are shown in Fig. 1. It was found that the titanium dioxide exists in the forms of anatase and the rutile. Since the anatase phase

Fig. 1 XRD spectra of the V₂O₅–TiO₂ layers synthesized under different applied voltages a 550, b 450, and c 350 V



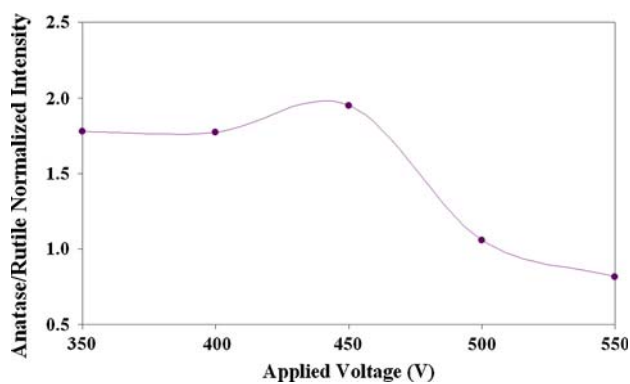
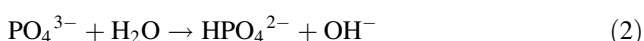


Fig. 2 Normalized anatase/rutile intensities as a function of the applied voltage

of TiO₂ is known for its photo-activity, the fraction of anatase in the synthesized layers determines the sample photo-catalytic performance. Therefore, the anatase/rutile normalized peak intensities were calculated from XRD patterns (Fig. 2). The results revealed that the anatase/rutile ratio reaches a maximum value at the applied voltage of 450 V and then decreases at higher voltages. Applying high voltages warms the anode up due to more electrical sparks taking place on the vicinity of the anode; meanwhile, the electrical current passing the cell increases with the applied voltage [31, 36]. Because of this extra heat, the anatase which is a meta-stable phase transforms to rutile stable phase at higher temperatures. A small shift toward higher 2θ s is observed in characteristic peaks of the anatase and the rutile phases when vanadia was loaded on titania. This shows that the lattice parameter decreases when V is incorporated in the titania lattice, and Ti is substituted by V. It should be reminded that the atomic radius of Ti (0.068 nm) is greater than that of V (0.052 nm). Because of this shift and the existence of V₂O₅ peaks, it can be concluded that the V₂O₅ is not only loaded on TiO₂ matrix but also doped in TiO₂ lattice. Both of these phenomena enhance the photo-catalytic performance of the layers, since the band gap energy is reduced due to the substitution of Ti by V; furthermore, when V₂O₅ is distributed on the TiO₂ matrix, both of them generate electron-hole pairs which are prerequisite for photo-catalytic reactions, and, hence, more e⁻-h⁺ pairs will be available.

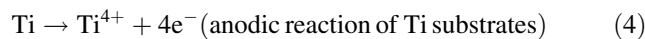
The following mechanism for formation of vanadia-titania composite layers by MAO process is put forward. At first, OH⁻ and VO₃⁻ anions are generated due to ionization of the sodium three-phosphate and sodium vanadate salts in the water:



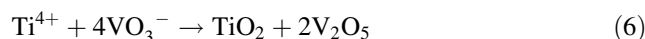
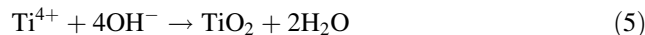
and



When the potential is applied (at the beginning time of the MAO process), titanium substrate, which is connected to the positive pole of the rectifier as anode, involves an oxidation reaction over the anode surface as below:



Simultaneously, the OH⁻ and VO₃⁻ anions move toward the anode surface because of the strong electrical field between anode and cathode, and react with the Ti⁴⁺ cations on the vicinity of the anode:



XPS technique, whose results are presented in Fig. 3, was used to further confirm the oxidation states of the titanium and vanadium elements in the composite layers. All of the binding energies were referenced to the C(1s) peak at 285.0 eV and interpreted according to the values reported by other scientists [44–46]. Figure 3a depicts the Ti(2p_{3/2}) core level binding energy. The peak located at the binding energy of 458.7 eV shows the existence of titanium in the form of Ti⁴⁺ state. The O(1s) peak, shown in Fig. 3b, can be resolved into two components using original XPS software. Both O(1s) peaks are wide and asymmetric demonstrating that there are at least two kind of O binding states in the layers. The peak A, located at 530.2 eV, is assigned to the crystal lattice oxygen (Ti–O and V–O), while the peak B, located at 531.7 eV, represents the oxygen in hydroxyl groups (O–H) from adsorbed water on the surface. Moreover, Fig. 3c shows V(2p_{3/2}) core level at binding energy of 517.6 eV corresponding to V⁵⁺ state indicating formation of V₂O₅.

Morphology of the layers synthesized under different voltages is depicted in Fig. 4. As is seen, no any pore was formed in the structure of the layers synthesized with applying voltages lower than the breakdown potential of the surface gas layer, as no electrical spark takes place at such voltages (Fig. 4a). It should be noted that the electrical discharges, which are responsible for pores formation, occur at the regions where the applied voltage on the anode surface is more than the breakdown potential of the gas layer enshrouding the anode [31, 36]. The electrical sparks are weak at low voltages due to low current passing the electrochemical cell; as a result, the structural pores are small at low applied voltages. In contrast, the electrical current increases at high applied voltages resulting in formation of wider pores due to stronger electrical sparks taking place on the vicinity of the anode.

Figure 5a illustrates the diffuse reflectance and $d\alpha/d\lambda$ as a function of the wavelength of the pure TiO₂ sample grown under 500 V applied voltage. Furthermore, the

Fig. 3 XPS spectra of the V_2O_5 - TiO_2 layer grown with applying 500 V **a** $Ti(2p_{3/2})$ core level, **b** $O(1s)$ core level, and **c** $V(2p_{3/2})$ core level binding energies

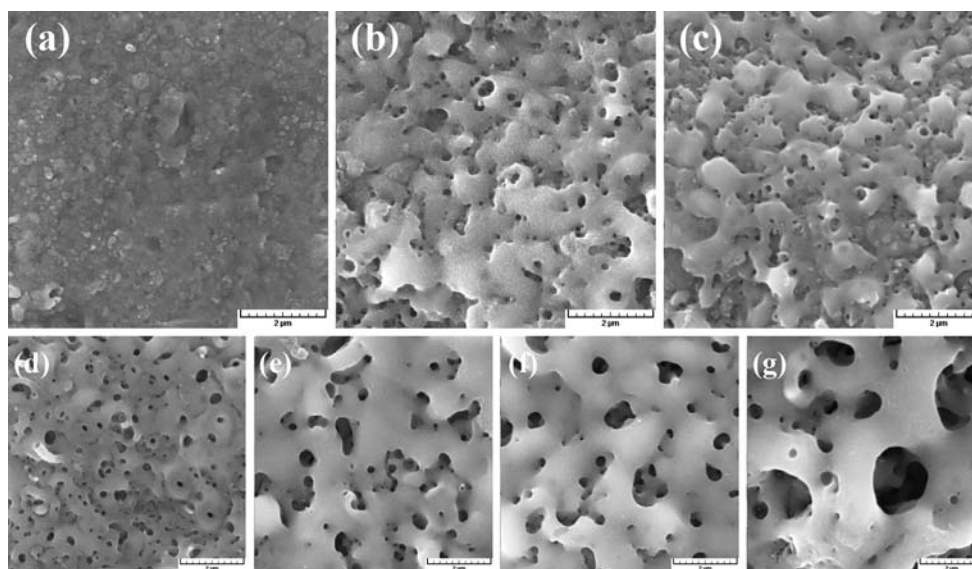
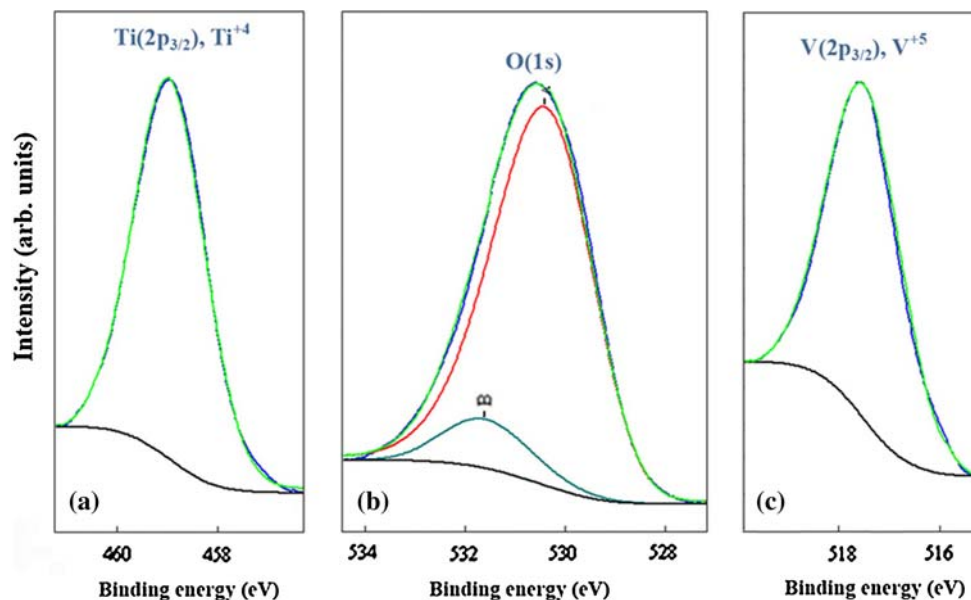


Fig. 4 Surface morphology of the V_2O_5 - TiO_2 layers grown under different applied voltages **a** 250, **b** 300, **c** 350, **d** 400, **e** 450, **f** 500, and **g** 550 V

diffuse reflectance and $d\alpha/d\lambda$ of the composite layer synthesized with applying 500 V is shown in Fig. 5b. Other results are not presented here. As is observed, the absorption edge of the layers shifted toward the visible region when V_2O_5 was introduced to TiO_2 . Mechanism of such a behavior can be found elsewhere [47–49]. According to the results, band gap energies of the pure TiO_2 and V_2O_5 - TiO_2 layers were calculated as 3.39 and 2.56 eV, respectively.

It has been reported that the photo-catalytic degradation of MB solution agrees with pseudo-first-order kinetics [50]. Consequently, the kinetic reaction rate constants (k) can be

calculated by the equation: $\ln(C/C_0) = -kt$ where C_0 is the concentration of the MB at $t = 0$, and C represents the concentration of MB at later times. In order to determine the photo-catalytic reaction rates (k), the quantity $\ln(C_0/C)$ was plotted as a function of irradiation time for different applied voltages. Figure 6a and b show the photo-catalytic performance of the pure TiO_2 and V_2O_5 - TiO_2 layers, respectively. It was observed that the photo-catalytic activity of the layers enhanced when vanadia was loaded on titania. Addition of V_2O_5 to TiO_2 creates apparently more redox sites and reduces the band gap energy of the

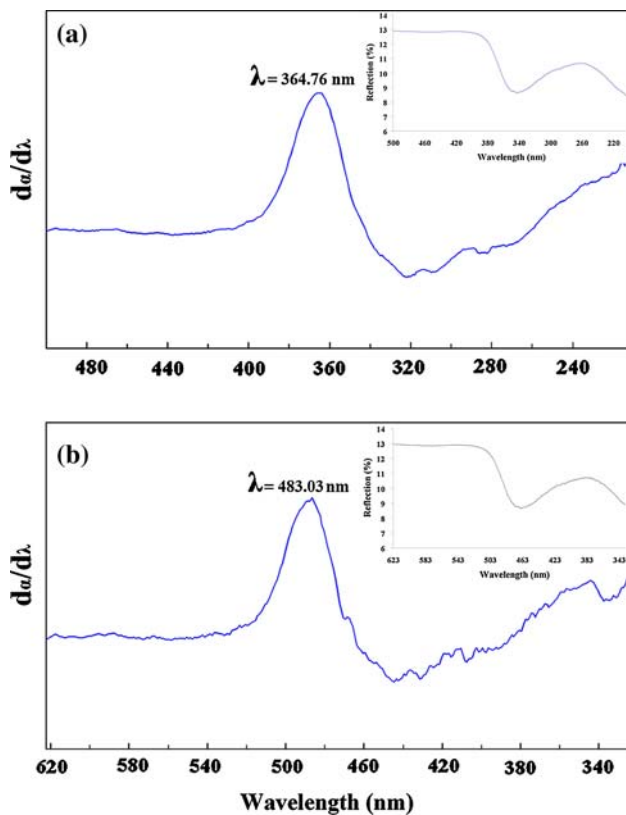


Fig. 5 Diffuse reflectance and $d\alpha/d\lambda$ versus wavelength for **a** pure TiO_2 and **b** V_2O_5 - TiO_2 layers

TiO_2 resulting in better photo-activity. It has also demonstrated that the surface of TiO_2 - V_2O_5 was more acidic than that of TiO_2 . The increased acidity can generate a higher affinity of TiO_2 - V_2O_5 for species with unpaired electrons; therefore, these films could absorb more OH^- or H_2O , and create more OH radical necessary for photo-oxidation reactions, resulting in enhancement of charge separation and photo-catalytic activity [11, 46]. In addition, the presence of OH radicals on the surface of the layers results in more attack to the MB molecules. Meanwhile, it was deduced that the photo-catalytic activity improved when applied voltage increased from 350 to 450 V, but reduced at the voltage of 550 V. The reason for such a behavior is that the anatase/rutile amount reaches its maximum value at the applied voltage of 450 V, as elucidated earlier.

4 Conclusions

V_2O_5 - TiO_2 porous layers were successfully synthesized by micro arc oxidation (MAO) process for the first time. The effect of the applied voltage on the surface morphology, phase structure, chemical composition, and photo-catalytic activity of the layers were studied. It was found the pore size increased with increasing the applied voltage. The

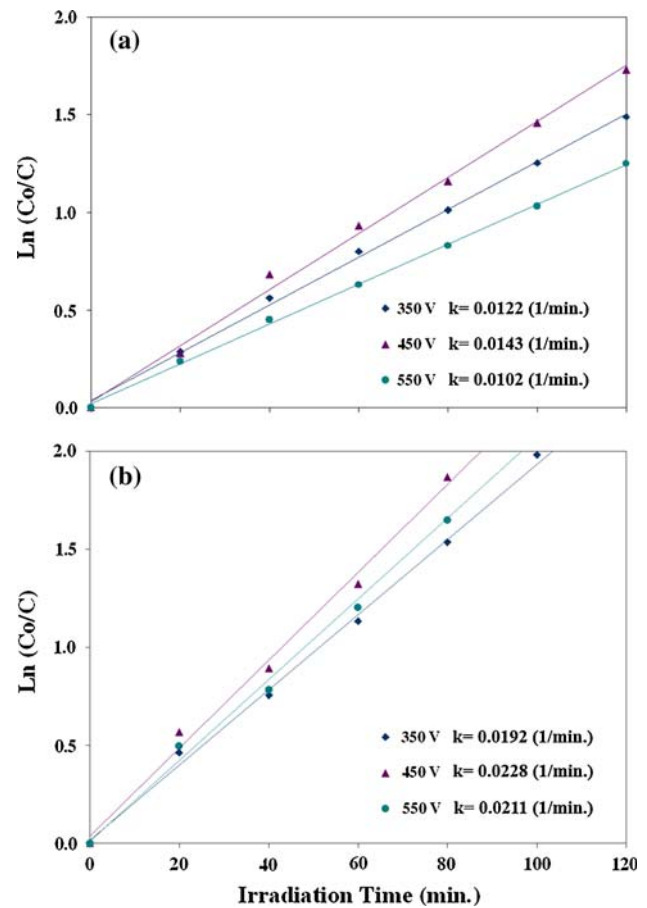


Fig. 6 $\ln(C_0/C)$ versus irradiation time for **a** TiO_2 and **b** V_2O_5 - TiO_2 layers

grown layers consisted of TiO_2 (in the forms of the anatase and the rutile phases) and V_2O_5 whose content varied with the applied voltage. It was also revealed that the absorption edge of the composite layers shifted toward the visible wavelengths when V_2O_5 was loaded on TiO_2 layers. It was also found that the composite layers had an improved photo-catalytic activity as compared with MAO-grown pure TiO_2 layers. About 92% of MB solution was decomposed over the produced composite layers surface after 120 min UV-irradiation.

Acknowledgments The authors would like to express their sincere thanks to all personnel in ceramic synthesis laboratory. The assistance of Mr. Rafi'ee for the XPS measurements is also appreciated.

References

1. Malik PK (2003) Dyes Pigment 56:239
2. Kumar KV, Ramamurthi V, Sivanesan S (2005) J Colloid Interface Sci 284:14
3. Vadivelan V, Kumar KV (2005) Equilibrium. J Colloid Interface Sci 286:90

4. Ravikumar K, Deebika B, Balu K (2005) *J Hazard Mater B* 122:75
5. Liou MJ, Lu MC, Chen JN (2003) *Water Res* 37:3172
6. Chatterjee D, Dasgupta S (2005) *J Photochem Photobiol C* 6:186
7. Ramaswamy V, Jagtap NB, Vijayanand S, Bhange DS, Awati PS (2008) *Mater Res Bull* 43:1145
8. Moshfegh AZ (2009) *J Phys D Appl Phys* 42:233001
9. Janus M, Kusiak E, Morawski AW (2009) *Catal Lett* 131:506
10. Fujishima A, Honda K (1972) *Nature* 238:37
11. Liu J, Fu Y, Sun Q, Shen J (2008) *Microporous Mesoporous Mater* 116:614
12. Sayilkan F, Asiltürk M, Kiraz N, Burunkaya E, Arpac E, Sayilkan H (2009) *J Hazard Mater* 162:1309
13. Anandan S, Kathiravan K, Murugesan V, Ikuma Y (2009) *Catal Commun* 10:1014
14. Bautista FM, Luna D, Luque J, Marinas JM, Sanchez-Royo JF (2009) *Appl Catal A General* 352:251
15. Moshfegh AZ, Ignatiev A (1990) *Catal Lett* 4:113
16. Yu C, Yu JC (2009) *Catal Lett* 129:462
17. Li X, Lv K, Deng K, Tang J, Su R, Sun J, Chen L (2009) *Mater Sci Eng B* 158:40
18. Trapalis CC, Keivanidis P, Kordas G, Zaharescu M, Crisan M, Sztatvanyi A, Gartner M (2003) *Thin Solid Films* 433:186
19. Zhang X, Yang H, Zhang F, Chan KY (2007) *Mater Lett* 61:2231
20. Li L, Liu CY, Liu Y (2009) *Mater Chem Phys* 113:551
21. Gu DE, Yang BC, Hu YD (2007) *Catal Lett* 118:254
22. Haber J, Nowak P, Zurek P (2008) *Catal Lett* 126:43
23. Minero C, Maririlla G, Maurino V, Pelizzetti E (2000) *Langmuir* 16:2632
24. Wang C, Bahnemann DF, Dohrmann JK (2000) *Chem Commun* 1539
25. Shou M, Takekawa H, Ju DY, Hagiwara T, Lu D, Tanaka K (2006) *Catal Lett* 108:119
26. Xu J, Sun K, Zhang L, Ren Y, Xu X (2006) *Catal Lett* 107:5
27. Ping Z, Mingxia X, Haibo F, Lingxia L (2009) *Mater Lett* 26
28. Tsumura T, Sogabe K, Toyoda M (2009) *Mater Sci Eng B* 157:113
29. Liu J, Yang R, Li S (2006) *Rare Met* 25:636
30. Ye FX, Tsumura T, Nakata K, Ohmori A (2008) *Mater Sci Eng B* 148:154
31. Yerokhin AL, Leyland A, Matthews A (2002) *Appl Surf Sci* 200:172
32. Jin F, Chu PK, Wang K, Zhao J, Huang A, Tong H (2008) *Mater Sci Eng A* 476:78
33. Wan L, Li JF, Feng JY, Sun W, Mao ZQ (2007) *Mater Sci Eng B* 139:216
34. Sun X, Jiang Z, Xin S, Yao Z (2005) *Thin Solid Films* 471:194
35. Gupta P, Tenhundfeld G, Daigle EO, Ryabkov D (2007) *Surf Coat Technol* 201:8746
36. Yerokhin AL, Nie X, Leyland A, Matthews A (2000) *Surf Coat Technol* 130:195
37. Li J, Wan L, Feng J (2009) *J Mater Proc Technol* 209:762
38. Yerokhin AL, Lyubimov VV, Ashitkov RV (1998) *Ceram Int* 24:1
39. Wang YM, Jiang BL, Lei TQ, Guo LX (2006) *Surf Coat Technol* 201:82
40. Yan Y, Han Y, Huang J (2008) *Scripta Mater* 59:203
41. Luo H, Cai Q, He J, Wei B (2009) *Curr Appl Phys* 9:1341
42. He J, Cai QZ, Ji YG, Luo HH, Li DJ, Yu B (2009) *J Alloys Compd* 482:476
43. Chang CC, Lin CK, Chan CC, Hsu CS, Chen CY (2006) *Thin Solid Films* 494:274
44. Machold T, Suprun WY, Papp H (2008) *J Mol Catal A Chem* 280:122
45. Moshfegh AZ, Ignatiev A (1991) *Thin Solid Films* 198:251
46. Zhao H, Bennici S, Shen J, Auroux A (2009) *Appl Catal A Gen* 356:121
47. Neatu S, Sacaliuc-Parvulescu E, Levy F, Parvulescu VI (2009) *Catal Today* 142:165
48. Tian B, Li C, Gu F, Jiang H, Hu Y, Zhang J (2009) *Chem Eng J* 151:220
49. Ge L, Xu M, Fang H (2006) *J Mol Catal A Chem* 258:68
50. An TC, Zhu XH, Xiong Y (2002) *Chemosphere* 46:897